Camelid single-domain antibodies raised by DNA immunization are potent inhibitors of EGFR signaling

Rossotti, Martin A.; Henry, Kevin A.; Van Faassen, Henk; Tanha, Jamshid; Callaghan, Deborah; Hussack, Greg; Arbabi-Ghahroudi, Mehdi; Mackenzie, C. Roger

Publisher's version / Version de l'éditeur:
https://doi.org/10.1042/BCJ20180795
Biochemical Journal, 2018-11-19

Camelid single-domain antibodies raised by DNA immunization are potent inhibitors of EGFR signaling

Martin A. Rossotti[1a], Kevin A. Henry[1a], Henk van Faassen[1], Jamshid Tanha[1,2], Deborah Callaghan[1], Greg Hussack[1], Mehdi Arbabi-Ghahroudi[1,3] and C. Roger MacKenzie[1*]

[1]Human Health Therapeutics Research Centre, National Research Council Canada, 100 Sussex Drive, Ottawa, Ontario, Canada, K1A 0R6

[2]Department of Biochemistry, Microbiology and Immunology, University of Ottawa, 451 Smyth Road, Ottawa, Ontario, Canada, K1H 8M5

[3]Department of Biology, Carleton University, 1125 Colonel By Drive, Ottawa, Ontario, Canada, K1S 5B6

[a]Equal contribution

*Address correspondence to:

C. Roger MacKenzie, Ph.D.

Human Health Therapeutics Research Centre, National Research Council Canada, 100 Sussex Drive, Ottawa, ON, Canada, K1A 0R6

Tel +1-613-990-0833 Fax +1-613-952-9092

roger.mackenzie@nrc-cnrc.gc.ca

Abstract word count: 213 Manuscript word count: 4,019

Abstract

Upregulation of epidermal growth factor receptor (**EGFR**) is a hallmark of many solid tumors, and inhibition of EGFR signaling by small molecules and antibodies has clear clinical benefit. Here, we report the isolation and functional characterization of novel camelid single-domain antibodies (**sdAbs** or **V_HHs**) directed against human EGFR. The source of these V_HHs was a llama immunized with cDNA encoding human EGFR ectodomain alone (no protein or cell boost), which is notable in that genetic immunization of large, outbred animals is generally poorly effective. The V_HHs targeted multiple sites on the receptor's surface with high affinity (K_D range: 1–40 nM), including one epitope overlapping that of cetuximab, several epitopes conserved in the cynomolgus EGFR orthologue, and at least one epitope conserved in the mouse EGFR orthologue. Interestingly, despite their generation against human EGFR expressed from cDNA by llama cells *in vivo* (presumably in native conformation), the V_HHs exhibited wide epitope-dependent variation in their apparent affinities for native EGFR displayed on tumor cell lines. As fusions to human IgG1 Fc, one of the V_HH-Fcs inhibited EGFR signaling induced by EGF binding with a potency similar to that of cetuximab (IC_{50}: ~30 nM). Thus, DNA immunization elicited high-affinity, functional sdAbs that were vastly superior to those previously isolated by our group through protein immunization.

Keywords: Antibody, single-domain antibody, V_HH, EGFR, cancer, DNA immunization

Introduction

The epidermal growth factor receptor (**EGFR**) is a receptor tyrosine kinase that is overexpressed and constitutively activated in up to 80% of solid cancers [1]. Following the development of small-molecule inhibitors, naked antibodies (**Abs**) against EGFR, exemplified by cetuximab, have shown clinical benefit in treating colorectal [2] and head and neck cancers [3], and other EGFR Abs are under investigation in other indications and as Ab-drug conjugates. Camelid single-domain antibodies (**sdAbs** or **V_HHs**) have previously been isolated against EGFR using protein immunization [4, 5] and whole-cell immunization [6, 7], and biparatopic molecules with improved potency have been constructed from these sdAb building blocks [8]. One advantage of sdAb-based biologics for cancer therapy is that they tend to penetrate solid tumors better than full-length IgGs [9].

DNA immunization of large outbred animals is generally recognized as inconsistent and poorly effective in eliciting humoral immune responses [10]. The mechanisms underlying this difficulty are thought to involve low rates of plasmid uptake and antigen expression, potentially relating to concentration effects in peripheral tissue. Six studies have examined DNA immunization of camelid species. In a study published in 2016, Peyrassol *et al.* [11] immunized four llamas with DNA encoding the G protein-coupled receptor (**GPCR**) ChemR23 by intradermal injection of plasmid DNA using a Dermojet® device, then boosted the animals with ChemR23-expressing Dubca cells; they observed ChemR23-specific Abs in the sera of only one of four llamas, and were able to isolate antagonistic sdAbs with apparent affinities for ChemR23-expressing cells of around 130–160 nM from phage display libraries constructed using the peripheral B-

68 cell repertoire of this animal. In a subsequent 2018 study, Peyrassol *et al.* [12]
69 immunized two llamas with DNA encoding the GPCR VPAC1, again by intradermal
70 injection of plasmid DNA followed by boosting with VPAC1-expressing CHO cells; they
71 did not describe the seroconversion of these animals, but were able to isolate sdAbs
72 with nM and µM apparent affinities for VPAC1-expressing cells from peripheral
73 repertoires. Van der Woning *et al.* [13] immunized four llamas with DNA encoding
74 glucagon receptor (GCGR) using intradermal injection followed by *in vivo*
75 electroporation, then boosted with GCGR-expressing Dubca cells. The authors claimed
76 that weak serum titers against GCGR were present in all four animals, although the
77 experiment was missing key controls (preimmune and irrelevant immune sera; irrelevant
78 antigens). Koch-Nolte *et al.* [14], Danquah *et al.* [15] and Fumey *et al.* [16] immunized
79 llamas with DNA encoding ART2.2, P2X7 and CD38, respectively, by biolistic
80 transfection using a Helios® gene gun system followed by boosting with either
81 recombinant protein or antigen-expressing cells. The off-rates of the anti-CD38 sdAbs
82 were consistent with binding affinities in the low-nM range. However, in these latter
83 three studies, neither serum analyses over the course of immunization nor per-animal
84 success rates were disclosed.
85 Here, we tested the hypothesis that high-affinity and functional camelid sdAbs
86 could be produced against a model antigen, EGFR, using DNA immunization alone. We
87 describe the comprehensive *in vitro* characterization of a panel of sdAbs generated in
88 this manner, which are dramatically superior to those we previously isolated using
89 protein immunization [4].
90

91 **Experimental**

92 *Antibodies and reagents*

93 Recombinant 6×His-tagged human EGFRvIII was produced by transient
94 transfection of HEK293-6E cells as previously described [17] and purified by
95 immobilized metal affinity chromatography (**IMAC**) followed by a final size exclusion
96 chromatography polishing step to remove aggregates. Recombinant 6×His-tagged
97 human EGFR ectodomain was from Genscript (Cat. No. Z03194; Piscataway, NJ),
98 recombinant *in vivo* biotinylated 6×His-tagged human EGFRvIII ectodomain was from
99 ACROBiosystems (Cat. No. EGR-H82E0; Newark, DE) and recombinant streptavidin
100 was from Thermo Fisher Scientific (Waltham, MA). Human EGFR-Fc fusion protein was
101 from Genscript (Cat. No. Z03381) and rhesus and mouse EGFR-Fc fusion proteins
102 were from Sino Biological (Cat. Nos. 90317-K02H and 51091-M02H; Beijing, China).
103 Horseradish peroxidase (**HRP**)-conjugated goat polyclonal anti-llama IgG was from
104 Cedarlane Labs (Cat. No. A160-100P; Burlington, Canada), HRP-conjugated goat
105 polyclonal anti-human IgG was from Sigma-Aldrich (St. Louis, MO) and 3,3',5,5'-
106 tetramethylbenzidine (**TMB**) substrate was from Mandel Scientific (Guelph, Canada).
107 Bovine serum albumin (**BSA**) and Tween-20 were from Sigma-Aldrich and all cell
108 culture reagents were from Thermo Fisher. Mouse monoclonal anti-c-Myc IgG was from
109 Santa Cruz Biotechnology (clone 9E10, Cat. No. sc-40; Dallas, TX), allophycocyanin
110 (**APC**)-conjugated goat polyclonal anti-mouse IgG was from Thermo Fisher (Cat. No.
111 A865), Alexa Fluor® 488 (**AF488**)-conjugated donkey anti-human IgG was from
112 Jackson ImmunoResearch (Cat. No. 709546098; West Grove, PA) and R-phycoerythrin
113 (**PE**)-conjugated streptavidin was from Thermo Fisher (Cat. No. S866). Erlotinib was

114 from Sigma-Aldrich, recombinant human epidermal growth factor (**EGF**) and mouse
115 monoclonal Ab against β-actin were from Genscript (Cat. Nos. Z00333 and A00702),
116 rabbit polyclonal Ab against phospho-EGFR (Tyr1068) was from Cell Signaling
117 Technology (Cat. No. 2234; Danvers, MA), mouse monoclonal Ab against human EGFR
118 was a generous gift from Anne Marcil (National Research Council Canada, Montréal,
119 Canada), and cetuximab was a generous gift from Yves Durocher (National Research
120 Council Canada, Montréal, Canada). HRP-conjugated donkey polyclonal anti-mouse
121 IgG was from Jackson ImmunoResearch (Cat. No. 715036150) and HRP-conjugated
122 goat polyclonal anti-rabbit IgG was from Cedarlane Labs (Cat. No. CLCC43007).
123 SuperSignal™ West Pico PLUS chemiluminescent substrate was from Thermo Fisher.
124 *Llama immunization*
125 A male llama (*Lama glama*) was immunized by biolistic transfection using a
126 Helios® gene gun system (Bio-Rad, Hercules, CA) followed by intradermal injection
127 using a DERMOJET device (AKRA DERMOJET, Pau, France). Two pTT5 vectors [17]
128 encoding either soluble human EGFRvIII (UniProt P00533: residues 1–29/Gly/297–645)
129 or membrane-tethered human EGFRvIII (UniProt P00533: residues 1–29/Gly/297–668)
130 were purified from overnight cultures of *Escherichia coli* DH5α cells using a QIAGEN®
131 Plasmid Maxi Kit (QIAGEN, Hilden, Germany). Briefly, 50 mg of gold particles were
132 coated with 100 µL of 0.05 M spermidine, then vortexed and sonicated. An equimolar
133 mixture of both pTT5 vectors (50 µg each; 100 µg total DNA in 100 µL ultrapure water)
134 was added to the spermidine-coated gold particles, then 100 µL of 1 M $CaCl_2$ was
135 added dropwise to the mixture. After incubating for 10 min at room temperature, the
136 gold particles were pelleted in a microfuge, washed three times with 100% ethanol, and

137 resuspended in 6 mL of 100% ethanol containing 0.05 mg/mL polyvinylpyrrolidone. The
138 DNA-gold solution was dried onto the inner walls of two 30-inch lengths of gold-coat
139 tubing under nitrogen flow, then the tubing was cut into 0.5-inch lengths.

140 The llama was immunized six times (weeks 0, 2, 4, 6, 9 and 12) by biolistic
141 transfection; each immunization consisted of 12 bombardments administered at 600 PSI
142 to shaved sites on the neck and hind limb (10 µg total DNA per immunization).
143 Thereafter, four additional immunizations (weeks 16, 20, 24 and 28) were administered
144 by intradermal injection of 1 mg (1 mg/mL) of DNA using a DERMOJET device. Serum
145 titration ELISA was conducted as described previously [18, 19] and binding was
146 detected using HRP-conjugated polyclonal goat anti-llama IgG. Experiments involving
147 animals were conducted using protocols approved by the National Research Council
148 Canada Animal Care Committee and in accordance with the guidelines set out in the
149 OMAFRA Animals for Research Act, R.S.O. 1990, c. A.22.

150 *Construction and panning of phage-displayed V_HH library*

151 A phage-displayed V_HH library was constructed from the peripheral blood
152 lymphocytes of the immunized llama as described previously [18-20]. Briefly, peripheral
153 blood mononuclear cells were purified by density gradient centrifugation from blood
154 obtained 5 days following the third and the final DERMOJET immunizations. Total RNA
155 was extracted from ~5×10^7 cells from each time point using a PureLink™ RNA Mini Kit
156 (Thermo Fisher) and cDNA was reverse transcribed using qScript® cDNA supermix
157 containing random hexamer and olido(dT) primers (Quanta Biosciences, Gaithersburg,
158 MD). V_HH genes were amplified using semi-nested PCR and cloned into the phagemid
159 vector pMED1 [20]; the final library had a size of 3×10^7 independent transformants and

160 an insert rate of approximately 75%. Phage particles were rescued from the library
161 using M13K07 helper phage and panned against microplate-adsorbed human EGFRvIII
162 for three rounds with trimethylamine elution as described previously [18-20]. A second
163 independent library selection was carried out in the same manner except that the target
164 was streptavidin-captured biotinylated EGFRvIII.

165 *Expression of V_HHs and V_HH-Fc fusions*

166 V_HH DNA sequences were cloned into the pSJF2H expression vector and
167 monomeric V_HHs tagged C-terminally with c-Myc and 6×His were purified from the
168 periplasm of *E. coli* TG1 cells by IMAC as previously described [18-20]. In addition, *in*
169 *vivo* biotinylated monomeric V_HHs were produced by co-transformation of *E. coli* BL21
170 (DE3) cells with two vectors encoding (i) V_HHs C-terminally tagged with a biotin
171 acceptor peptide and 6×His and (ii) the biotin ligase BirA and purified by IMAC [21].
172 Bivalent V_HH-human IgG1 Fc fusions were produced by transient transfection of
173 HEK293-6E cells followed by protein A affinity chromatography as previously described
174 [17, 22]. Heterodimeric biparatopic V_HH-Fc fusions were produced by co-transfection of
175 HEK293-6E cells with two pTT5 vectors encoding (i) NRC-sdAb032-Fc tagged C-
176 terminally with 6×His and (ii) a second untagged V_HH-Fc. The heterodimeric Ab was
177 purified by sequential protein A affinity chromatography and IMAC and eluted using a
178 linear 0→0.5 M imidazole gradient over 20 column volumes to separate species bearing
179 one or two 6×His tags. V_HHs and V_HH-Fcs were dialyzed against or buffer-exchanged
180 into phosphate-buffered saline (**PBS**), pH 7.4.

181 *ELISA and EGF-competition ELISA*

182 Wells of NUNC® MaxiSorp™ microtiter plates (Thermo Fisher) were coated
183 overnight at 4°C with 2 µg/mL streptavidin in 100 µL of PBS, pH 7.4. The wells were
184 blocked with 200 µL of PBS containing 1% (w/v) BSA for 1 h at 37°C, then biotinylated
185 V_HHs (10 µg/mL in 100 µL of PBS containing 1% BSA and 0.1% (v/v) Tween-20) were
186 captured for 30 min at room temperature. The wells were washed 5× with PBS
187 containing 0.1% Tween-20 and then incubated with human EGFR-Fc (500 ng/mL in 100
188 µL of PBS containing 1% BSA and 0.05% Tween-20) in the presence or absence of
189 EGF (17 µg/mL) for 1 h at room temperature. The wells were washed 5× again and
190 incubated with HRP-conjugated goat anti-human IgG (1 µg/mL in 100 µL of PBS
191 containing 1% BSA and 0.05% Tween-20) for 1 h at room temperature. After a final
192 wash (5× with PBS containing 0.1% Tween-20), the wells were developed with TMB
193 substrate, stopped with 1 M H_2SO_4 and the absorbance at 450 nm was measured using
194 a Multiskan™ FC photometer (Thermo Fisher).
195 *Surface plasmon resonance*
196 Prior to surface plasmon resonance (**SPR**) analyses, monomeric V_HHs were
197 purified by preparative size exclusion chromatography using a Superdex™ 75 10/300
198 GL column (GE Healthcare, Piscataway, NJ) connected to an ÄKTA FPLC protein
199 purification system (GE Healthcare). In the first SPR experiment, multi-cycle kinetic
200 analyses were performed on a Biacore™ 3000 instrument (GE Healthcare) at 25°C in
201 HBS-EP buffer (10 mM HEPES, pH 7.4, containing 150 mM NaCl, 3 mM EDTA, and
202 0.005% (w/v) surfactant P20). Approximately 1304–2158 and 741 resonance units
203 (**RUs**), respectively, of recombinant human EGFR and EGFRvIII ectodomains were
204 immobilized on a CM5 sensor chip (GE Healthcare) in 10 mM acetate buffer, pH 4.5,

205 using an amine coupling kit (GE Healthcare). An ethanolamine-blocked flow cell served
206 as the reference. Monomeric V_HHs at concentrations ranging from 0.1 nM – 100 nM
207 were injected over the EGFR and EGFRvIII surfaces in HBS-EP buffer at a flow rate of
208 20 µL/min. For NRC-sdAb032 only, the V_HH (212 RUs) was immobilized on a CM5
209 sensor chip by amine coupling and 0.5 nM – 50 nM recombinant human EGFR
210 ectodomain was injected over the V_HH surface in HBS-EP buffer at a flow rate of 20
211 µL/min. Contact times were 180–300 s and dissociation times were 300–600 s. The
212 EGFR, EGFRvIII and NRC-sdAb032 surfaces were regenerated using a 10-s pulse of
213 10 mM glycine, pH 1.5.

214 In the second SPR experiment, single-cycle kinetic analyses were performed on
215 a Biacore™ T200 instrument (GE Healthcare) at 25°C in HBS-EP buffer. Approximately
216 618, 1051 and 600 RUs of human, rhesus and mouse EGFR-Fc, respectively, were
217 immobilized on three flow cells of a Series S Sensor Chip CM5 (GE Healthcare) in 10
218 mM acetate buffer, pH 4.5, using an amine coupling kit. An ethanolamine-blocked flow
219 cell served as the reference. Monomeric V_HHs at concentrations ranging from 0.6 nM –
220 50 nM were injected over the EGFR surfaces in HBS-EP buffer at a flow rate of 40
221 µL/min. The contact time was 180 s and the dissociation time was 600 s. The EGFR
222 surfaces were regenerated using a 10-s pulse of 10 mM glycine, pH 1.5.

223 Epitope binning experiments were performed essentially as described above on
224 a Biacore™ 3000 instrument, except that 3383 RUs of human EGFR-Fc were
225 immobilized on a CM5 sensor chip. A single V_HH (or cetuximab) at a concentration
226 equivalent to 25× K_D was injected at 40 µL/min with a contact time of 150 s to saturate
227 the EGFR surface. The second injection consisted of the same V_HH (or cetuximab) in

228 the presence of 25× the K_D concentration of a second V_HH. All data were analyzed by
229 fitting to a 1:1 interaction model using BIAevaluation 4.1 software (GE Healthcare).
230 *Flow cytometry and mirrorball® assays*
231 MDA-MB-468 and MCF7 cells were cultured at 37°C in a humidified 5% CO_2
232 atmosphere in T75 flasks containing RPMI-1640 medium supplemented with 10% (v/v)
233 FBS, 2 mM glutamine, 100 U/mL penicillin, 100 µg/mL streptomycin and 250 ng/mL
234 amphotericin B. For flow cytometry experiments, cells were grown to 70–80%
235 confluency, dissociated using trypsin-EDTA solution, washed in PBS and then
236 resuspended in PBS containing 1% BSA. Approximately 1×10^5 cells were stained
237 sequentially on ice for 30 min with: (i) 20 µg/mL of each V_HH, (ii) 5 µg/mL of mouse anti-
238 c-Myc IgG, and (iii) 5 µg/mL of APC-conjugated goat anti-mouse IgG. The cells were
239 washed with PBS in between each staining step, and after a final wash, data were
240 acquired on a BD FACSCanto™ instrument (BD Biosciences, San Jose, CA).
241 For mirrorball® experiments, cells were dissociated from flasks using Accutase®
242 solution, washed in Hank's Balanced Salt Solution (**HBSS**) and then approximately
243 5,000 cells in growth medium were plated in each rat tail collagen-coated well of a
244 Nunc™ MicroWell 96-well optical bottom plate (Thermo Fisher). After incubating at
245 37°C/5% CO_2 for 24 h, the cells were washed with HBSS and Abs (biotinylated V_HHs,
246 V_HH-Fcs or cetuximab, serially diluted in live cell imaging buffer (LCIB) containing 1%
247 BSA) were added to wells for 2 h at 4°C. The cells were washed with LCIB and
248 secondary detection reagents (40 µg/mL PE-conjugated streptavidin or 30 µg/mL
249 AF488-conjugated donkey anti-human IgG in LCIB containing 1% BSA) were added as
250 appropriate to each well for 1 h at 4°C. The cells were washed with LCIB and stained

251 with 1 µM DRAQ5™ for 10 min at 4°C. After a final wash with LCIB, data were acquired
252 on a mirrorball® microplate cytometer (TTP Labtech, Melbourn, UK) and analyzed using
253 Cellista software (TTP Labtech).

254 *EGFR phosphorylation assay*

255 Approximately 2×10^5 MDA-MB-468 cells were seeded in wells of 12-well tissue
256 culture plates and then starved in serum-free RPMI-1640 medium overnight. The next
257 day, the medium was replaced with RPMI-1640 containing 1% BSA and various
258 concentrations of erlotinib or Abs (V_HH-Fcs or cetuximab). After 30 min at 37°C, EGF
259 was added to a final concentration of 25 nM and incubated for a further 15 min. The
260 cells were cooled immediately on ice, washed twice with PBS and then scraped in 100
261 µL Laemmli buffer. Cell lysates (5 µL) were electrophoresed on 4–20% Mini-Protean®
262 TGX™ precast gels (Bio-Rad Laboratories, Hercules, CA) and transferred to
263 polyvinylidene fluoride membranes using the semi-dry method. Western blotting was
264 performed as previously described [6]. Briefly, membranes were blocked overnight at
265 4°C with 2% BSA in PBS, then sequentially incubated for 1 h at room temperature with:
266 (i) primary Abs (anti-phospho-EGFR, anti-EGFR or anti-β-actin, all diluted 1:1,500 in
267 PBS containing 1% BSA and 0.1% Tween-20) and (ii) secondary Abs (HRP-conjugated
268 donkey anti-mouse IgG or goat anti-rabbit IgG, diluted 1:3,000 in PBS containing 1%
269 BSA and 0.1% Tween-20). The membranes were washed extensively with PBS
270 containing 0.1% Tween-20 following incubations with primary and secondary Abs. The
271 blots were developed using enhanced chemiluminescence and imaged using a
272 Molecular Imager® Gel Doc™ XR+ System (Bio-Rad Laboratories). Band densitometry
273 analysis was conducted using ImageJ version 1.52.

274 *V_HH humanization*

275 V_HHs were humanized by alignment with human IGHV3-30*01 and IGHJ1-1*01
276 amino acid sequences. For each V_HH, three humanized variants were designed
277 representing a spectrum of increasing homology to the human germline: (i) variant H1,
278 in which all FR sequences were reverted to the human consensus excepting residues
279 located within five positions of a FR-CDR boundary; (ii) variant H2, in which all FR
280 sequences were reverted to the human consensus excepting residues located within
281 two positions of a FR-CDR boundary; and (iii) variant H3, in which all FR sequences
282 were fully human. CDR residues as well as FR2 positions 42 and 52 (IMGT numbering)
283 were left unaltered in all variants.

284

Results and Discussion

Llama DNA immunization using gene gun and DERMOJET

We immunized a llama with DNA encoding human EGFRvIII six times every 2–3 weeks by biolistic transfection using a gene gun. No polyclonal serum Ab response was evident in the animal following the six gene gun immunizations, but boosting three times by intradermal injection using a DERMOJET device elicited serum Abs against recombinant EGFR with a half-maximal titer of approximately 1:5,000 (**Fig. 1**). Binding of polyclonal serum Abs to EGFR and EGFRvIII was roughly equivalent and was not improved by further boosting.

V_HHs elicited by DNA immunization targeted five unique EGFR epitopes including an epitope overlapping that of cetuximab

A phage-displayed V_HH library was constructed from the peripheral blood lymphocytes of the immunized llama and V_HHs were isolated by panning against either plate-adsorbed EGFRvIII or streptavidin-captured biotinylated EGFRvIII. Ten unique V_HHs falling into three sequence families were identified in the panning against plate-adsorbed EGFRvIII (NRC-sdAb021 – NRC-sdAb030; **Supplementary Table S1**); all of these V_HHs as well as two others (NRC-sdAb032 and NRC-sdAb033) were identified by panning against streptavidin-captured biotinylated EGFRvIII. The V_HHs had monovalent binding affinities for recombinant human EGFR, ranging from 1 nM – 40 nM as measured by SPR, and, despite immunization with DNA encoding EGFRvIII, all showed identical binding to EGFR and EGFRvIII (**Fig. 2A**, **Table 1**). In contrast with a previous report, we measured the EGFR-binding affinity of EG2 (a V_HH raised by immunization with recombinant EGFRvIII ectodomain) as approximately 15–20 nM, not 55 nM [4]. The

308 V_HHs showed a variety of cross-species reactivity patterns (**Table 2** and
309 **Supplementary Fig. S1**): EG2 V_HH bound only human EGFR, NRC-sdAb022-family
310 V_HHs and NRC-sdAb032 bound human and rhesus EGFR with similar affinity, and
311 NRC-sdAb029-family V_HHs and NRC-sdAb033 bound human, rhesus and mouse EGFR
312 with similar affinity. Surprisingly, NRC-sdAb028 bound human and mouse EGFR with
313 similar affinity but did not react with rhesus EGFR. SPR epitope binning co-injection
314 experiments showed that: (i) EG2 V_HH recognized a distinct epitope present only on
315 human EGFR; (ii) NRC-sdAb029-family V_HHs recognized a distinct epitope conserved
316 across human, rhesus and mouse EGFR; (iii) NRC-sdAb022-family V_HHs and NRC-
317 sdAb028 recognized highly overlapping but distinct epitopes (conserved across human
318 and rhesus EGFR and human, rhesus and mouse EGFR, respectively) while NRC-
319 sdAb033 recognized a partially-overlapping but highly conserved epitope; and (iv) NRC-
320 sdAb032 recognized an epitope partially overlapping that of cetuximab (**Fig. 2B** and
321 **Supplementary Fig. S2**). NRC-sdAb032 shared further similarities with cetuximab, in
322 that both Abs cross-reacted with rhesus but not mouse EGFR, neither Ab bound well in
323 SPR to immobilized EGFR but did bind EGFR in solution (data not shown), and both
324 Abs competed with EGF for EGFR binding (**Fig. 2C**).
325 Despite their broadly similar monovalent affinities for recombinant EGFR (1 nM –
326 40 nM), the V_HHs showed significant variability in their ability to recognize EGFR-
327 positive tumor cell lines. Flow cytometry showed that four of five epitope bins targeted
328 by the V_HH monomers were accessible on native cell-surface EGFR; neither binding of
329 NRC-sdAb029 nor, surprisingly, binding of EG2 to MDA-MB-468 cells was detectable at
330 single concentration (20 µg/mL, equivalent to approximately 1.3 µM) in this assay (**Fig.**

331 **3A**). Titration of the V_HH-Fc fusions against adherent MDA-MB-468 cells in mirrorball®
332 microplate cytometry assay revealed very weak binding of EG2-Fc (EC_{50}: 279 nM),
333 moderate binding of NRC-sdAb022-Fc, NRC-sdAb028-Fc and NRC-sdAb033-Fc
334 (EC_{50}s: 67 nM, 86 nM and 49 nM, respectively) and strong binding of NRC-sdAb032
335 (EC_{50}: 0.5 nM, similar to cetuximab) (**Fig. 3B**). Similar binding patterns were observed
336 for *in vivo* biotinylated V_HH monomers (data not shown), and no binding of either the
337 V_HHs or V_HH-Fcs was observed to EGFR-low MCF7 cells (**Fig. 3C**). Binding by
338 biparatopic heterodimeric V_HH/V_HH-Fcs combining NRC-sdAb032 with each of the other
339 possible V_HHs was similar to the parental homodimeric NRC-sdAb032-Fc (**Fig. 3D**),
340 suggesting that monovalent interaction of the NRC-sdAb032 V_HH arm with EGFR drove
341 the majority of binding in this assay. Thus, almost all of the V_HHs raised by DNA
342 immunization recognized native EGFR on tumor cells better than EG2 V_HH, and one
343 V_HH-Fc (NRC-sdAb032-Fc) had an EC_{50} 1–2 logs lower than previously reported V_HHs
344 (in bivalent form) raised by recombinant protein immunization [4, 6].

345 *NRC-sdAb032, a V_HH elicited by DNA immunization, inhibited EGFR signaling with*
346 *potency similar to cetuximab*

347 We tested the ability of all of the V_HH-Fcs showing significant binding to EGFR-
348 positive tumor cells (NRC-sdAb022-Fc, NRC-sdAb028-Fc, NRC-sdAb032-Fc and NRC-
349 sdAb033-Fc), as well as cetuximab and EG2-Fc as a historical control, to inhibit EGF-
350 induced EGFR phosphorylation. At a single concentration of 500 nM, NRC-sdAb032-Fc
351 was the only V_HH-Fc showing significant inhibition of EGFR signaling (**Fig 4A, B**).
352 Reduction of EGFR phosphorylation in the presence of NRC-sdAb032-Fc was dose-
353 dependent, with an IC50 between 25–50 nM, similar to that of cetuximab (**Fig. 4C, D**).

354 No improvement in potency was achieved by biparatopic heterodimeric V_HH/V_HH-Fcs
355 combining NRC-sdAb032 with each other V_HH, although there appeared to be a general
356 advantage of molecules bearing two EGFR-binding arms (other than EG2) over
357 V_HH/V_HH-Fcs bearing a single EGFR-binding arm (**Fig. 4E, F**).

358 *Humanization of V_HHs*

359 With the aim of using these V_HHs in therapeutic applications, the sequences of
360 the four V_HHs showing significant binding to EGFR-positive tumor cells (NRC-sdAb022,
361 NRC-sdAb028, NRC-sdAb032 and NRC-sdAb033) were humanized with reference to
362 human IGHV3-30*01 and IGHJ1*01 germline genes. This process yielded at least one
363 humanized variant with unimpaired solubility and EGFR-binding affinity for three of the
364 four parent V_HHs (NRC-sdAb028-H1, NRC-sdAb032-H1, NRC-sdAb033-H2). The
365 framework regions of these humanized variants bore 89–94% sequence identity with
366 human IGHV3-30*01, with no or minimal impact on the biophysical properties and
367 EGFR-binding affinities of the resulting V_HHs (**Table 3** and **Supplementary Table S2**).

368 *Conclusions and implications*

369 The V_HHs isolated and characterized here were generated by immunization of a
370 llama with DNA alone (no protein or cell boost), using biolistic transfection (gene gun)
371 followed by intradermal injection (DERMOJET). Many of the V_HHs had high affinities for
372 recombinant human EGFR, cross-reacted with rhesus and/or mouse EGFR, and
373 recognized native cell-surface EGFR on tumor cell lines; in all of these respects, the
374 V_HHs described here are dramatically superior to those previously isolated by our group
375 using recombinant protein immunization [4]. One V_HH, NRC-sdAb032, showed clear
376 functional activity as an inhibitor of EGFR signaling, and any of the humanized V_HHs

377 may have other therapeutic applications. NRC-sdAb032 was isolated by panning on
378 streptavidin-captured EGFR but not on passively-adsorbed EGFR, and its epitope
379 appears to be present on native EGFR and recombinant EGFR ectodomain in solution
380 but not on the same ectodomain when it is passively adsorbed to microtiter plates or
381 amine coupled to sensor chips. This epitope, which overlaps the cetuximab epitope and
382 the EGF-binding site in EGFR domain III, is apparently poorly available for binding by
383 NRC-sdAb032 or cetuximab in ELISAs against directly-adsorbed EGFR or in SPR
384 experiments in which these antibodies are flowed over amine-coupled EGFR surfaces;
385 by contrast, both NRC-sdAb032 and cetuximab bound $EGFR^+$ tumor cells with lower
386 $EC50_s$ than other V_HHs with similar monovalent binding affinities for recombinant EGFR.
387 We speculate that the NRC-sdAb032 epitope, though easily destroyed, contributes to
388 this V_HH's superior recognition of native EGFR displayed on the tumor cell surface.
389 Other groups have had similar experiences using streptavidin-captured antigens as
390 'bait' during panning of phage-displayed V_HH libraries [23].
391 We are currently investigating whether the DNA immunization schedule
392 presented here is consistent and generalizable to other targets. Our preliminary findings
393 have indicated that up to five intradermal injections alone were unable to elicit a
394 polyclonal serum Ab response against EGFR in several other llamas, and thus one
395 possibility is that either a prolonged immunization schedule or a combination of two
396 immunization routes (particle bombardment; intradermal injection) may be necessary to
397 trigger seroconversion. These hypotheses are under investigation (Mehdi Arbabi-
398 Ghahroudi, in preparation), although evaluating the impact of immunization strategies in

399 the context of the significant heterogeneity expected in large outbred animals is a major
400 challenge.

401 **Acknowledgements**

402 We gratefully acknowledge the excellent technical help of Yonghong Guan, Hong
403 Tong-Sevinc, Qingling Yang, and Shalini Raphael. This work was supported by funding
404 from the National Research Council Canada.

405

406 **Author Contributions**

407 KAH, CRM and MAG designed the immunization study. KAH performed serology
408 and built the phage-displayed V_HH library. KAH and MAR isolated V_HHs by panning.
409 HvF and GH conducted surface plasmon resonance experiments. DC performed
410 mirrorball® experiments. MAR produced V_HH-Fc fusions and performed western blotting
411 experiments to assess EGFR phosphorylation status. KAH and GH made the figures
412 and KAH wrote the paper. JT and MAG proofread the text. All authors approved the
413 final manuscript.

414

415 **Additional Information**

416 *Competing Financial Interests*

417 None to declare.

418 **References**

419 1 Herbst, R. S. and Shin, D. M. (2002) Monoclonal antibodies to target epidermal
420 growth factor receptor-positive tumors: a new paradigm for cancer therapy. Cancer. **94**,
421 1593-1611

422 2 Jonker, D. J., O'Callaghan, C. J., Karapetis, C. S., Zalcberg, J. R., Tu, D., Au, H.
423 J., Berry, S. R., Krahn, M., Price, T., Simes, R. J., Tebbutt, N. C., van Hazel, G.,
424 Wierzbicki, R., Langer, C. and Moore, M. J. (2007) Cetuximab for the treatment of
425 colorectal cancer. N Engl J Med. **357**, 2040-2048

426 3 Bonner, J. A., Harari, P. M., Giralt, J., Azarnia, N., Shin, D. M., Cohen, R. B.,
427 Jones, C. U., Sur, R., Raben, D., Jassem, J., Ove, R., Kies, M. S., Baselga, J.,
428 Youssoufian, H., Amellal, N., Rowinsky, E. K. and Ang, K. K. (2006) Radiotherapy plus
429 cetuximab for squamous-cell carcinoma of the head and neck. N Engl J Med. **354**, 567-
430 578

431 4 Bell, A., Wang, Z. J., Arbabi-Ghahroudi, M., Chang, T. A., Durocher, Y., Trojahn,
432 U., Baardsnes, J., Jaramillo, M. L., Li, S., Baral, T. N., O'Connor-McCourt, M.,
433 Mackenzie, R. and Zhang, J. (2010) Differential tumor-targeting abilities of three single-
434 domain antibody formats. Cancer Lett. **289**, 81-90

435 5 Gottlin, E. B., Xiangrong, G., Pegram, C., Cannedy, A., Campa, M. J. and Patz,
436 E. F., Jr. (2009) Isolation of novel EGFR-specific VHH domains. J Biomol Screen. **14**,
437 77-85

438 6 Roovers, R. C., Laeremans, T., Huang, L., De Taeye, S., Verkleij, A. J., Revets,
439 H., de Haard, H. J. and van Bergen en Henegouwen, P. M. (2007) Efficient inhibition of

440 EGFR signaling and of tumour growth by antagonistic anti-EFGR Nanobodies. Cancer
441 Immunol Immunother. **56**, 303-317
442 7 Salema, V., Manas, C., Cerdan, L., Pinero-Lambea, C., Marin, E., Roovers, R.
443 C., Van Bergen En Henegouwen, P. M. and Fernandez, L. A. (2016) High affinity
444 nanobodies against human epidermal growth factor receptor selected on cells by E. coli
445 display. MAbs. **8**, 1286-1301
446 8 Roovers, R. C., Vosjan, M. J., Laeremans, T., el Khoulati, R., de Bruin, R. C.,
447 Ferguson, K. M., Verkleij, A. J., van Dongen, G. A. and van Bergen en Henegouwen, P.
448 M. (2011) A biparatopic anti-EGFR nanobody efficiently inhibits solid tumour growth. Int
449 J Cancer. **129**, 2013-2024
450 9 Niu, G., Murad, Y. M., Gao, H., Hu, S., Guo, N., Jacobson, O., Nguyen, T. D.,
451 Zhang, J. and Chen, X. (2012) Molecular targeting of CEACAM6 using antibody probes
452 of different sizes. J Control Release. **161**, 18-24
453 10 Babiuk, L. A., Pontarollo, R., Babiuk, S., Loehr, B. and van Drunen Littel-van den
454 Hurk, S. (2003) Induction of immune responses by DNA vaccines in large animals.
455 Vaccine. **21**, 649-658
456 11 Peyrassol, X., Laeremans, T., Gouwy, M., Lahura, V., Debulpaep, M., Van
457 Damme, J., Steyaert, J., Parmentier, M. and Langer, I. (2016) Development by Genetic
458 Immunization of Monovalent Antibodies (Nanobodies) Behaving as Antagonists of the
459 Human ChemR23 Receptor. J Immunol. **196**, 2893-2901
460 12 Peyrassol, X., Laeremans, T., Lahura, V., Debulpaep, M., El Hassan, H.,
461 Steyaert, J., Parmentier, M. and Langer, I. (2018) Development by Genetic
462 Immunization of Monovalent Antibodies Against Human Vasoactive Intestinal Peptide

463 Receptor 1 (VPAC1), New Innovative, and Versatile Tools to Study VPAC1 Receptor
464 Function. Front Endocrinol (Lausanne). **9**, 153
465 13 van der Woning, B., De Boeck, G., Blanchetot, C., Bobkov, V., Klarenbeek, A.,
466 Saunders, M., Waelbroeck, M., Laeremans, T., Steyaert, J., Hultberg, A. and De Haard,
467 H. (2016) DNA immunization combined with scFv phage display identifies antagonistic
468 GCGR specific antibodies and reveals new epitopes on the small extracellular loops.
469 MAbs. **8**, 1126-1135
470 14 Koch-Nolte, F., Reyelt, J., Schossow, B., Schwarz, N., Scheuplein, F.,
471 Rothenburg, S., Haag, F., Alzogaray, V., Cauerhff, A. and Goldbaum, F. A. (2007)
472 Single domain antibodies from llama effectively and specifically block T cell ecto-ADP-
473 ribosyltransferase ART2.2 in vivo. FASEB J. **21**, 3490-3498
474 15 Danquah, W., Meyer-Schwesinger, C., Rissiek, B., Pinto, C., Serracant-Prat, A.,
475 Amadi, M., Iacenda, D., Knop, J. H., Hammel, A., Bergmann, P., Schwarz, N.,
476 Assuncao, J., Rotthier, W., Haag, F., Tolosa, E., Bannas, P., Boue-Grabot, E., Magnus,
477 T., Laeremans, T., Stortelers, C. and Koch-Nolte, F. (2016) Nanobodies that block
478 gating of the P2X7 ion channel ameliorate inflammation. Sci Transl Med. **8**, 366ra162
479 16 Fumey, W., Koenigsdorf, J., Kunick, V., Menzel, S., Schutze, K., Unger, M.,
480 Schriewer, L., Haag, F., Adam, G., Oberle, A., Binder, M., Fliegert, R., Guse, A., Zhao,
481 Y. J., Cheung Lee, H., Malavasi, F., Goldbaum, F., van Hegelsom, R., Stortelers, C.,
482 Bannas, P. and Koch-Nolte, F. (2017) Nanobodies effectively modulate the enzymatic
483 activity of CD38 and allow specific imaging of CD38(+) tumors in mouse models in vivo.
484 Sci Rep. **7**, 14289

485 17 Durocher, Y., Perret, S. and Kamen, A. (2002) High-level and high-throughput
486 recombinant protein production by transient transfection of suspension-growing human
487 293-EBNA1 cells. Nucleic Acids Res. **30**, E9
488 18 Henry, K. A., Hussack, G., Collins, C., Zwaagstra, J. C., Tanha, J. and
489 MacKenzie, C. R. (2016) Isolation of TGF-beta-neutralizing single-domain antibodies of
490 predetermined epitope specificity using next-generation DNA sequencing. Protein Eng
491 Des Sel. **29**, 439-443
492 19 Henry, K. A., Tanha, J. and Hussack, G. (2015) Identification of cross-reactive
493 single-domain antibodies against serum albumin using next-generation DNA
494 sequencing. Protein Eng Des Sel. **28**, 379-383
495 20 Baral, T. N., MacKenzie, R. and Arbabi Ghahroudi, M. (2013) Single-domain
496 antibodies and their utility. Curr Protoc Immunol. **103**, Unit 2 17
497 21 Rossotti, M. A., Pirez, M., Gonzalez-Techera, A., Cui, Y., Bever, C. S., Lee, K.
498 S., Morisseau, C., Leizagoyen, C., Gee, S., Hammock, B. D. and Gonzalez-Sapienza,
499 G. (2015) Method for Sorting and Pairwise Selection of Nanobodies for the
500 Development of Highly Sensitive Sandwich Immunoassays. Anal Chem. **87**, 11907-
501 11914
502 22 Zhang, J., Liu, X., Bell, A., To, R., Baral, T. N., Azizi, A., Li, J., Cass, B. and
503 Durocher, Y. (2009) Transient expression and purification of chimeric heavy chain
504 antibodies. Protein Expr Purif. **65**, 77-82
505 23 Pardon, E., Laeremans, T., Triest, S., Rasmussen, S. G., Wohlkonig, A., Ruf, A.,
506 Muyldermans, S., Hol, W. G., Kobilka, B. K. and Steyaert, J. (2014) A general protocol
507 for the generation of Nanobodies for structural biology. Nat Protoc. **9**, 674-693

508 24 Hussack, G., Arbabi-Ghahroudi, M., van Faassen, H., Songer, J. G., Ng, K. K.,
509 MacKenzie, R. and Tanha, J. (2011) Neutralization of Clostridium difficile toxin A with
510 single-domain antibodies targeting the cell receptor binding domain. J Biol Chem. **286**,
511 8961-8976

512

513

514

515 **Table 1. Monovalent affinities of V_HHs for recombinant human EGFR and EGFRvIII**
516 **extracellular domains (pH 7.4, 25°C)**

V_HH	EGFR			EGFRvIII		
	k_{on} ($M^{-1}s^{-1}$)	k_{off} (s^{-1})	K_D (nM)	k_{on} ($M^{-1}s^{-1}$)	k_{off} (s^{-1})	K_D (nM)
EG2	1.1×10^{6}	2.8×10^{-2}	19.1	1.2×10^{6}	1.7×10^{-2}	14.6
NRC-sdAb021	3.1×10^{5}	1.2×10^{-2}	38.5	2.4×10^{5}	9.8×10^{-3}	40.4
NRC-sdAb022	4.0×10^{5}	6.7×10^{-4}	1.7	2.9×10^{5}	7.7×10^{-4}	2.6
NRC-sdAb023	4.6×10^{5}	5.7×10^{-3}	12.6	3.4×10^{5}	6.7×10^{-3}	19.4
NRC-sdAb024	2.5×10^{5}	7.3×10^{-4}	2.9	1.8×10^{5}	9.0×10^{-4}	4.9
NRC-sdAb025	3.6×10^{5}	5.9×10^{-4}	1.7	2.6×10^{5}	7.1×10^{-4}	2.8
NRC-sdAb026	3.6×10^{5}	5.6×10^{-3}	15.4	2.7×10^{5}	6.8×10^{-3}	25.0
NRC-sdAb027	5.1×10^{5}	7.9×10^{-4}	1.6	3.8×10^{5}	8.6×10^{-4}	2.3
NRC-sdAb028	8.4×10^{4}	7.5×10^{-4}	9.0	9.8×10^{4}	8.4×10^{-4}	8.6
NRC-sdAb029	4.0×10^{5}	4.0×10^{-3}	9.9	4.4×10^{5}	4.4×10^{-3}	10.2
NRC-sdAb030	2.7×10^{5}	5.9×10^{-3}	21.4	2.9×10^{5}	6.6×10^{-3}	22.7
NRC-sdAb032	1.0×10^{5}	1.3×10^{-3}	12.9[a]	n.d.[b]	n.d.[b]	n.d.[b]
NRC-sdAb033	1.5×10^{5}	1.7×10^{-4}	1.1	n.d.[b]	n.d.[b]	n.d.[b]

517 [a]Determined by amine-coupling NRC-sdAb032 and flowing recombinant EGFR ectodomain

518 [b]No difference was observed in ELISA binding to human EGFR or EGFRvIII (data not shown)

519 n.d., not determined

520

521 **Table 2. Monovalent affinities and kinetics of the interaction between V_HHs and**
522 **human, rhesus and mouse EGFR-Fc (pH 7.4, 25°C).**

V_HH	Human EGFR-Fc			Rhesus EGFR-Fc			Mouse EGFR-Fc		
	k_{on} ($M^{-1}s^{-1}$)	k_{off} (s^{-1})	K_D (nM)	k_{on} ($M^{-1}s^{-1}$)	k_{off} (s^{-1})	K_D (nM)	k_{on} ($M^{-1}s^{-1}$)	k_{off} (s^{-1})	K_D (nM)
EG2	8.5×10^{5}	8.5×10^{-3}	11.1±0.2	-	-	-	-	-	-
NRC-sdAb022	2.5×10^{5}	2.2×10^{-3}	8.9±0.1	8.5×10^{4}	1.7×10^{-3}	19.6±0.7	-	-	-
NRC-sdAb028	9.2×10^{4}	5.5×10^{-4}	6.0±0.1	-	-	-	6.5×10^{5}	7.5×10^{-3}	11.6±0.3
NRC-sdAb029	5.3×10^{5}	4.5×10^{-3}	8.5±0.1	5.5×10^{5}	6.4×10^{-3}	11.8±0.3	5.1×10^{5}	6.3×10^{-3}	12.5±1.2
NRC-sdAb032	3.6×10^{5}	2.5×10^{-3}	6.9±0.02	4.8×10^{5}	3.9×10^{-3}	8.1±0.1	-	-	-
NRC-sdAb033	9.0×10^{4}	1.6×10^{-4}	1.8±0.1	1.1×10^{5}	1.1×10^{-4}	1.0±0.1	9.2×104	2.8×10^{-4}	3.1±0.2

523 (-) indicates no binding

524 K_D values are expressed as the means ± standard deviations of three independent experiments

525

526

527 **Table 3**. Aggregation propensities and monovalent affinities of humanized V_HHs for
528 human EGFR-Fc.

V_HH	Monomer (%)[a]	k_{on} ($M^{-1}s^{-1}$)	k_{off} (s^{-1})	K_D (nM)
NRC-sdAb022	>95	2.5×10^5	2.2×10^{-3}	8.9±0.1
NRC-sdAb022-H1	n.d.[a]			
NRC-sdAb022-H2	<50	n.b.[b]	n.b.[b]	n.b.[b]
NRC-sdAb022-H3	n.d.			
NRC-sdAb028	>95	9.2×10^4	5.5×10^{-4}	6.0±0.1
NRC-sdAb028-H1	>95	9.3×10^4	5.8×10^{-4}	6.2±0.2
NRC-sdAb028-H2	n.d.			
NRC-sdAb028-H3	n.d.			
NRC-sdAb032	>95	3.6×10^5	2.5×10^{-3}	6.9±0.02
NRC-sdAb032-H1	>95	6.2×10^5	1.0×10^{-2}	16.6±0.5
NRC-sdAb032-H2	<50	n.d.[c]	n.d.[c]	254±31
NRC-sdAb032-H3	n.d.			
NRC-sdAb033	>95	9.0×10^4	1.6×10^{-4}	1.8±0.1
NRC-sdAb033-H1	>95	1.3×10^5	2.2×10^{-4}	1.7±0.03
NRC-sdAb033-H2	>95	2.0×10^5	2.6×10^{-4}	1.4±0.1
NRC-sdAb033-H3	<50	1.3×10^5	1.1×10^{-2}	83.8±3.7

529 [b]Determined by SEC (% monomer peak area).

530 [b]n.d., not determined due to low or no expression.

531 [c]n.b., no binding of the purified monomeric sdAb to human EGFR-Fc could be detected.

532 [d]n.d., not determined because steady-state K_D was calculated.

533 **Figure Legends**

534

535 **Figure 1.** Serum titration ELISA of the immunized llama against recombinant human
536 EGFR and human EGFRvIII ectodomains. Wells of NUNC® MaxiSorp™ microtiter plates
537 were coated overnight at 4°C with 100 ng of EGFR or EGFRvIII in 35 µL of PBS. The
538 wells were blocked with 200 µL of PBS containing 2% skim milk for 1 h at 37°C, then
539 sera (serially diluted in PBS containing 1% BSA and 0.1% Tween-20) were added to
540 wells for 2 h at room temperature. The wells were washed 5× with PBS containing 0.1%
541 Tween-20, incubated for 1 h with HRP-conjugated goat anti-llama IgG (diluted 1:5,000
542 in PBS containing 1% BSA and 0.1% Tween-20), washed 5× again and then developed
543 with TMB substrate.

544 **Figure 2**. Binding of V_HHs to EGFR by SPR and ELISA. **(A)** SPR sensorgrams showing
545 single-cycle kinetic analysis of V_HH binding to human EGFR-Fc. Recombinant EGFR-Fc
546 was immobilized on a Series S Sensor Chip CM5 using amine coupling, then the
547 indicated V_HH was flowed over the surface at concentrations ranging from 0.6 nM – 50
548 nM (NRC-sdAb022, 1.5 nM – 25 nM; NRC-sdAb028, 1.5 nM – 25 nM; NRC-sdAb029,
549 1.5 nM – 25 nM; NRC-sdAb032, 3 nM – 50 nM; NRC-sdAb033, 0.6 nM – 10 nM; EG2, 3
550 nM – 50 nM). Black lines show data and red lines show fits. **(B)** Summary of epitope
551 binning by SPR. The colors of the circles indicate the cross-species conservation of the
552 epitope (red, human EGFR only; blue, human and rhesus EGFR; yellow, human and
553 mouse EGFR; green, human, rhesus and mouse EGFR). **(C)** Competitive ELISA
554 showing binding of V_HHs to EGFR in the presence or absence of EGF.

555

556 **Figure 3**. Binding of V_HHs to EGFR-positive MDA-MB-431 cells and EGFR-low MCF7
557 cells. **(A)** Binding of V_HH monomers (20 µg/mL) to EGFR-positive MDA-MB-431 cells by
558 flow cytometry detected using anti-c-Myc and AF647-labeled anti-mouse antibodies. **(B,**
559 **C)** Binding of serially diluted V_HH-Fcs to EGFR-positive MDA-MB-431 cells **(B)** and
560 EGFR-low MCF7 cells **(C)** by mirrorball® microplate cytometry detecting using AF488-
561 labeled anti-human Fc antibody. EC_{50}s were determined by curve fitting in Graphpad
562 Prism using the equation for one-site specific binding with Hill slope. **(D)** Binding of
563 serially diluted biparatopic V_HH-Fcs by mirrorball® microplate cytometry detecting using
564 AF488-labeled anti-human Fc antibody. EC_{50}s were determined by curve fitting in
565 Graphpad Prism using the equation for one-site specific binding with Hill slope.

566

567 **Figure 4**. Inhibition of EGF-induced EGFR phosphorylation in MDA-MB-468 cells by
568 V_HH-Fcs. **(A)** Western blotting of phosphorylated EGFR (Tyr1068), total EGFR and β-
569 actin in serum-starved MDA-MB-468 cells treated with EGF in the presence or absence
570 of the indicated inhibitor (all at 500 nM). **(B)** Densitometry analysis of bands in A. **(C)**
571 Western blotting of phosphorylated EGFR (Tyr1068), bulk EGFR and β-actin in serum-
572 starved MDA-MB-468 cells treated with EGF in the presence or absence of the
573 indicated concentration of inhibitor. **(D)** Densitometry analysis of bands in C. The
574 concentrations used are as shown in C. A20.1-Fc is an irrelevant V_HH-Fc against
575 *Clostridium difficile* toxin A [24] included as a negative control. **(E)** Western blotting of
576 phosphorylated EGFR (Tyr1068), total EGFR and β-actin in serum-starved MDA-MB-

577 468 cells treated with EGF in the presence or absence of the indicated inhibitor (all at 5

578 nM). **(F)** Densitometry analysis of bands in E.

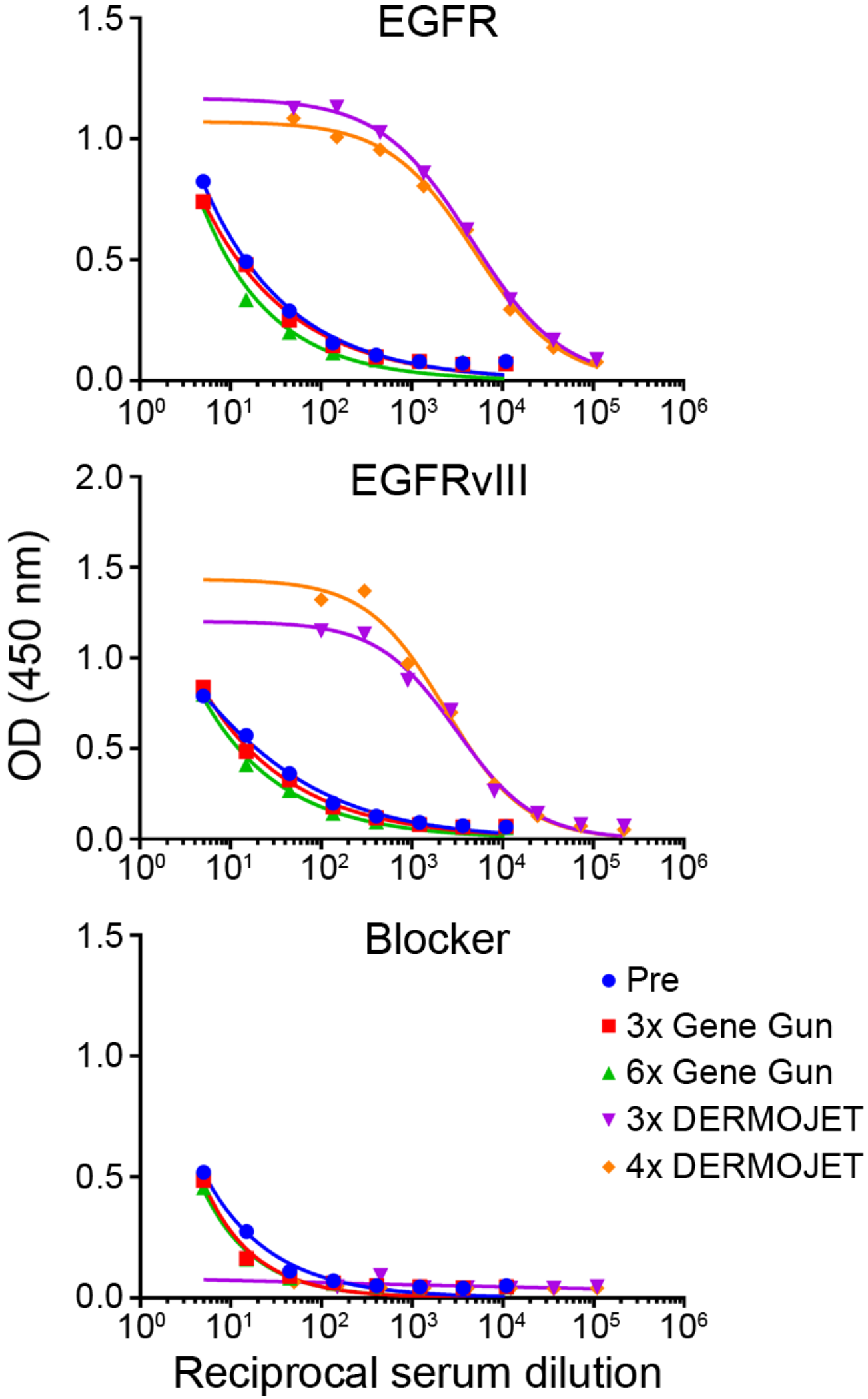
EGFR
EGFRvIII
Blocker
OD (450 nm)
Reciprocal serum dilution
Pre
3x Gene Gun
6x Gene Gun
3x DERMOJET
4x DERMOJET
0.0
0.5
1.0
1.5
2.0
10^0
10^1
10^2
10^3
10^4
10^5
10^6

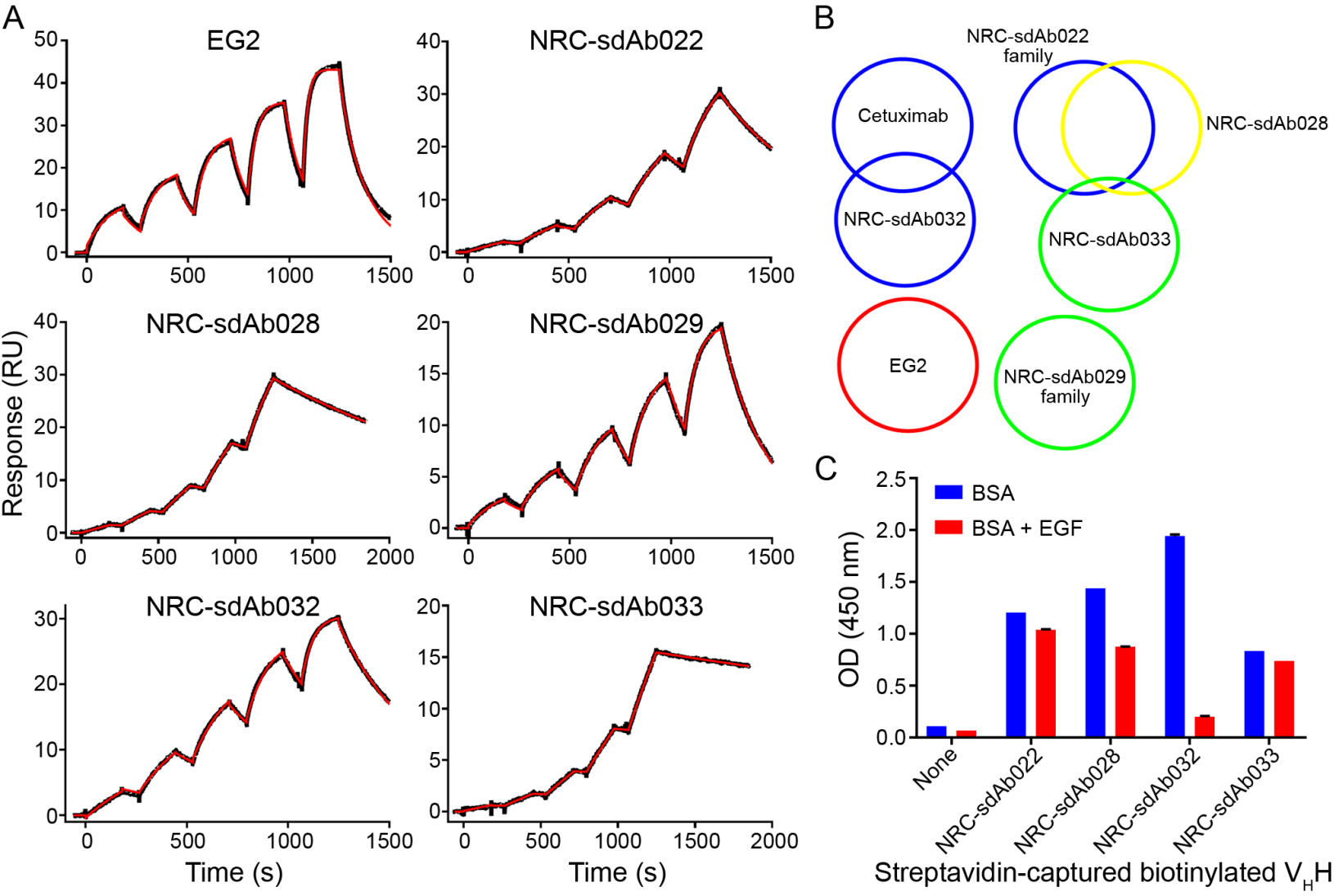
A
EG2
NRC-sdAb022
NRC-sdAb028
NRC-sdAb029
NRC-sdAb032
NRC-sdAb033
Response (RU)
Time (s)
Time (s)
B
NRC-sdAb022 family
Cetuximab
NRC-sdAb028
NRC-sdAb032
NRC-sdAb033
EG2
NRC-sdAb029 family
C
BSA
BSA + EGF
OD (450 nm)
None
NRC-sdAb022
NRC-sdAb028
NRC-sdAb032
NRC-sdAb033
Streptavidin-captured biotinylated V_HH

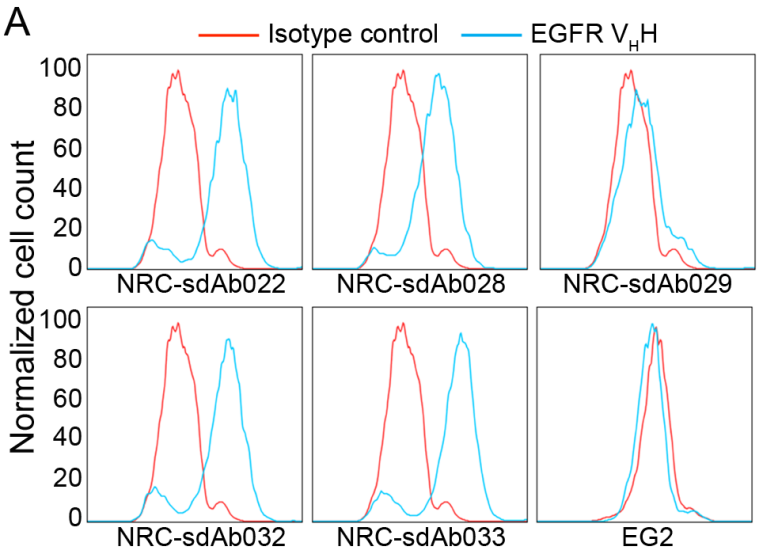
A
Isotype control
EGFR V_HH
Normalized cell count
100
80
60
40
20
0
NRC-sdAb022
NRC-sdAb028
NRC-sdAb029
NRC-sdAb032
NRC-sdAb033
EG2

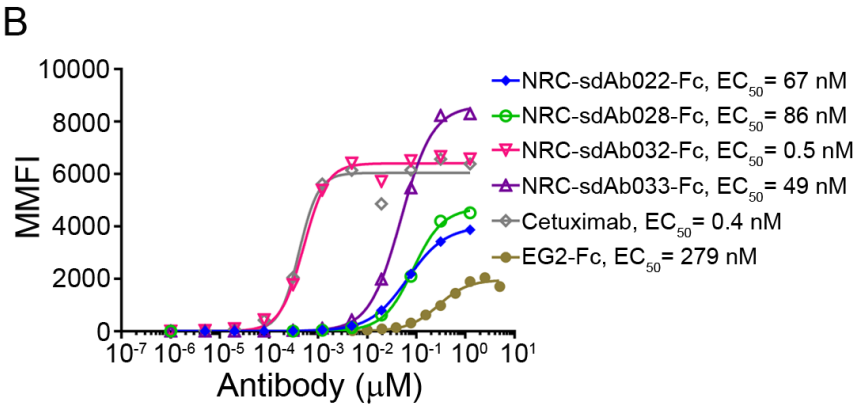
B
MMFI
10000
8000
6000
4000
2000
0
10^{-7} 10^{-6} 10^{-5} 10^{-4} 10^{-3} 10^{-2} 10^{-1} 10^{0} 10^{1}
Antibody (μM)
NRC-sdAb022-Fc, EC_{50}= 67 nM
NRC-sdAb028-Fc, EC_{50}= 86 nM
NRC-sdAb032-Fc, EC_{50}= 0.5 nM
NRC-sdAb033-Fc, EC_{50}= 49 nM
Cetuximab, EC_{50}= 0.4 nM
EG2-Fc, EC_{50}= 279 nM

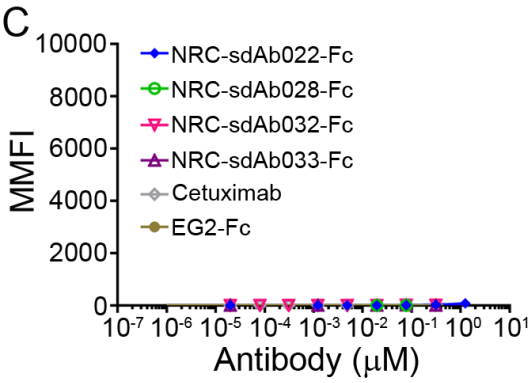
C
MMFI
10000
8000
6000
4000
2000
0
10^{-7} 10^{-6} 10^{-5} 10^{-4} 10^{-3} 10^{-2} 10^{-1} 10^{0} 10^{1}
Antibody (μM)
NRC-sdAb022-Fc
NRC-sdAb028-Fc
NRC-sdAb032-Fc
NRC-sdAb033-Fc
Cetuximab
EG2-Fc

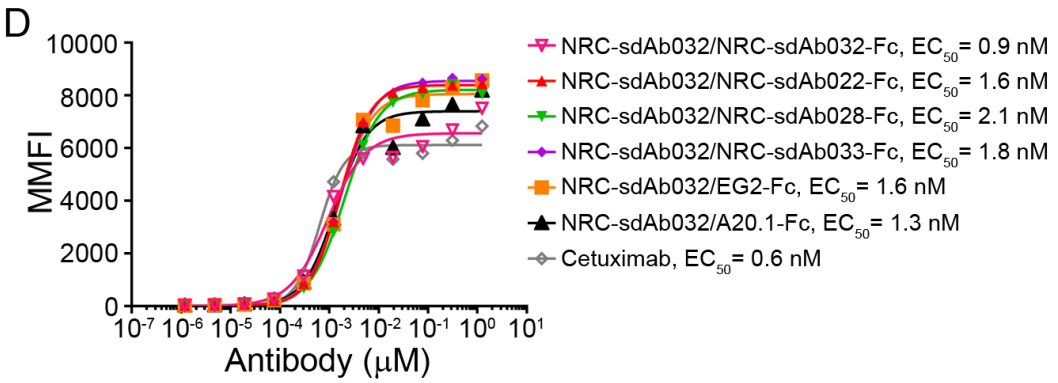
D
MMFI
10000
8000
6000
4000
2000
0
10^{-7} 10^{-6} 10^{-5} 10^{-4} 10^{-3} 10^{-2} 10^{-1} 10^{0} 10^{1}
Antibody (μM)
NRC-sdAb032/NRC-sdAb032-Fc, EC_{50}= 0.9 nM
NRC-sdAb032/NRC-sdAb022-Fc, EC_{50}= 1.6 nM
NRC-sdAb032/NRC-sdAb028-Fc, EC_{50}= 2.1 nM
NRC-sdAb032/NRC-sdAb033-Fc, EC_{50}= 1.8 nM
NRC-sdAb032/EG2-Fc, EC_{50}= 1.6 nM
NRC-sdAb032/A20.1-Fc, EC_{50}= 1.3 nM
Cetuximab, EC_{50}= 0.6 nM

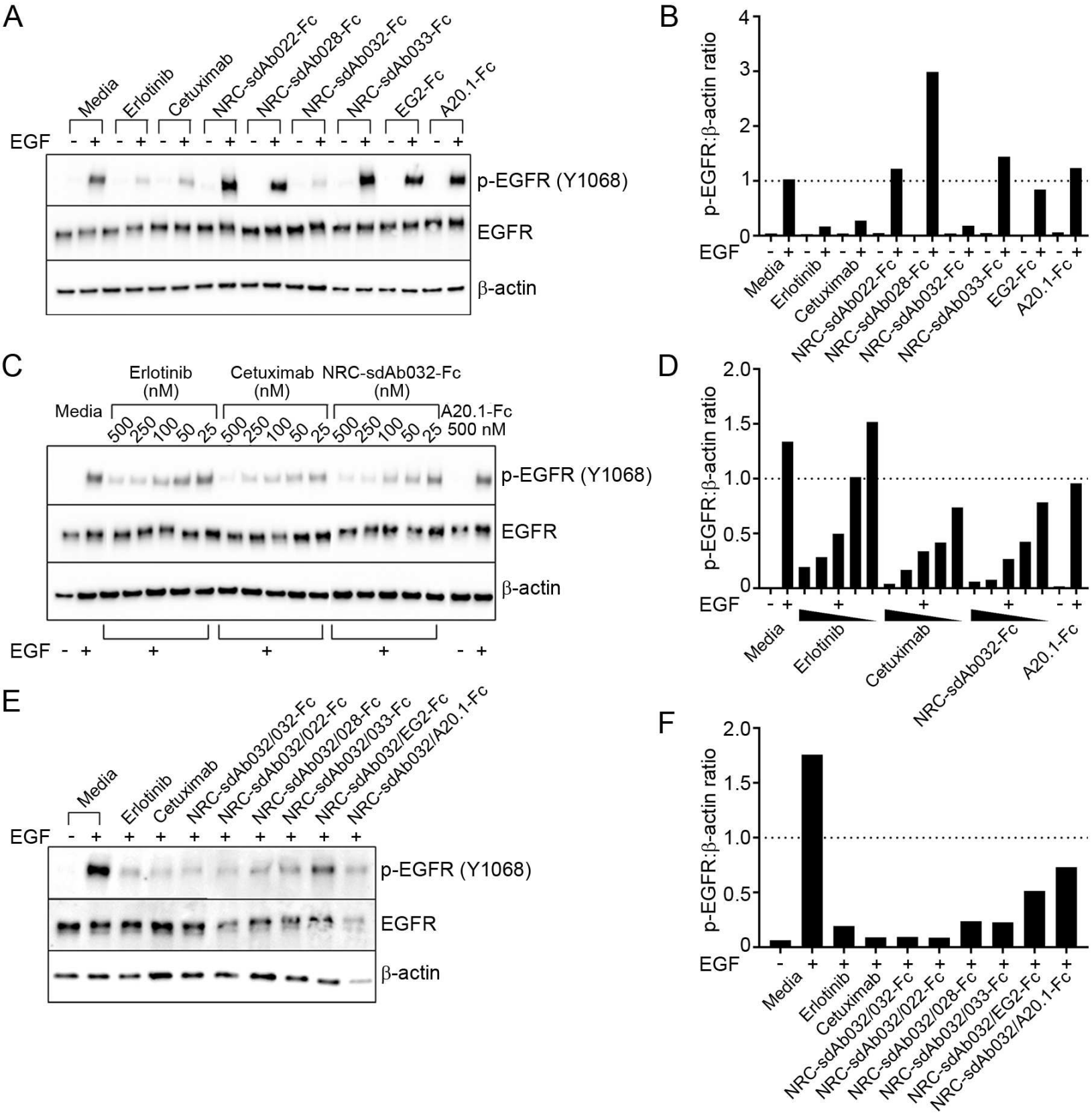
A
Media
Erlotinib
Cetuximab
NRC-sdAb022-Fc
NRC-sdAb028-Fc
NRC-sdAb032-Fc
NRC-sdAb033-Fc
EG2-Fc
A20.1-Fc
EGF
p-EGFR (Y1068)
EGFR
β-actin
B
p-EGFR:β-actin ratio
C
Erlotinib (nM)
Cetuximab (nM)
NRC-sdAb032-Fc (nM)
500 250 100 50 25
A20.1-Fc 500 nM
D
E
NRC-sdAb032/032-Fc
NRC-sdAb032/022-Fc
NRC-sdAb032/028-Fc
NRC-sdAb032/033-Fc
NRC-sdAb032/EG2-Fc
NRC-sdAb032/A20.1-Fc
F

Supplementary Material

Camelid single-domain antibodies raised by DNA immunization are potent inhibitors of EGFR signaling

Martin A. Rossotti[1a], Kevin A. Henry[1a], Henk van Faassen[1], Jamshid Tanha[1,2], Deborah Callaghan[1], Greg Hussack[1], Mehdi Arbabi-Ghahroudi[1,3] and C. Roger MacKenzie[1*]

[1]Human Health Therapeutics Research Centre, National Research Council Canada, 100 Sussex Drive, Ottawa, Ontario, Canada, K1A 0R6

[2]Department of Biochemistry, Microbiology and Immunology, University of Ottawa, 451 Smyth Road, Ottawa, Ontario, Canada, K1H 8M5

[3]Department of Biology, Carleton University, 1125 Colonel By Drive, Ottawa, Ontario, Canada, K1S 5B6

[a]Equal contribution

*Address correspondence to:

C. Roger MacKenzie, Ph.D.

Human Health Therapeutics Research Centre, National Research Council Canada, 100 Sussex Drive, Ottawa, ON, Canada, K1A 0R6

Tel +1-613-990-0833 Fax +1-613-952-9092

.

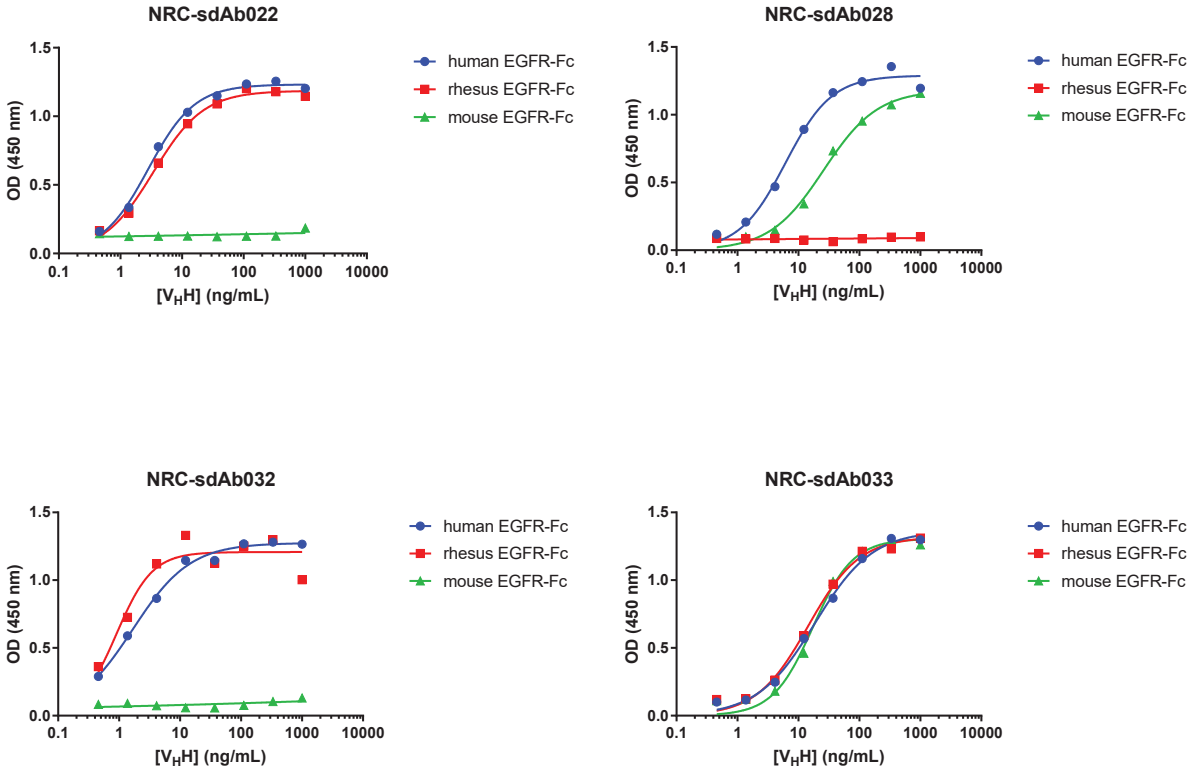

Supplementary Figure S1. Binding of V_HHs elicited by DNA immunization to human, rhesus and mouse EGFR-Fc in ELISA. Wells of Nunc® MaxiSorp™ microtiter plates were coated with 100 ng of each EGFR-Fc in 35 µL PBS overnight at 4°C. The next day, wells were blocked with 200 µL of 2% (w/v) skim milk in PBS for 1 h at 37°C. Antibodies were serially diluted in PBS containing 1% (w/v) BSA and 0.1% (v/v) Tween-20 and added to wells for 2 h at room temperature. The wells were washed 5× with PBS containing 0.1% Tween-20, incubated for 1 h with HRP-conjugated rabbit anti-6×His antibody (Cedarlane Labs), washed 5× again and then developed with TMB substrate as described in the main text.

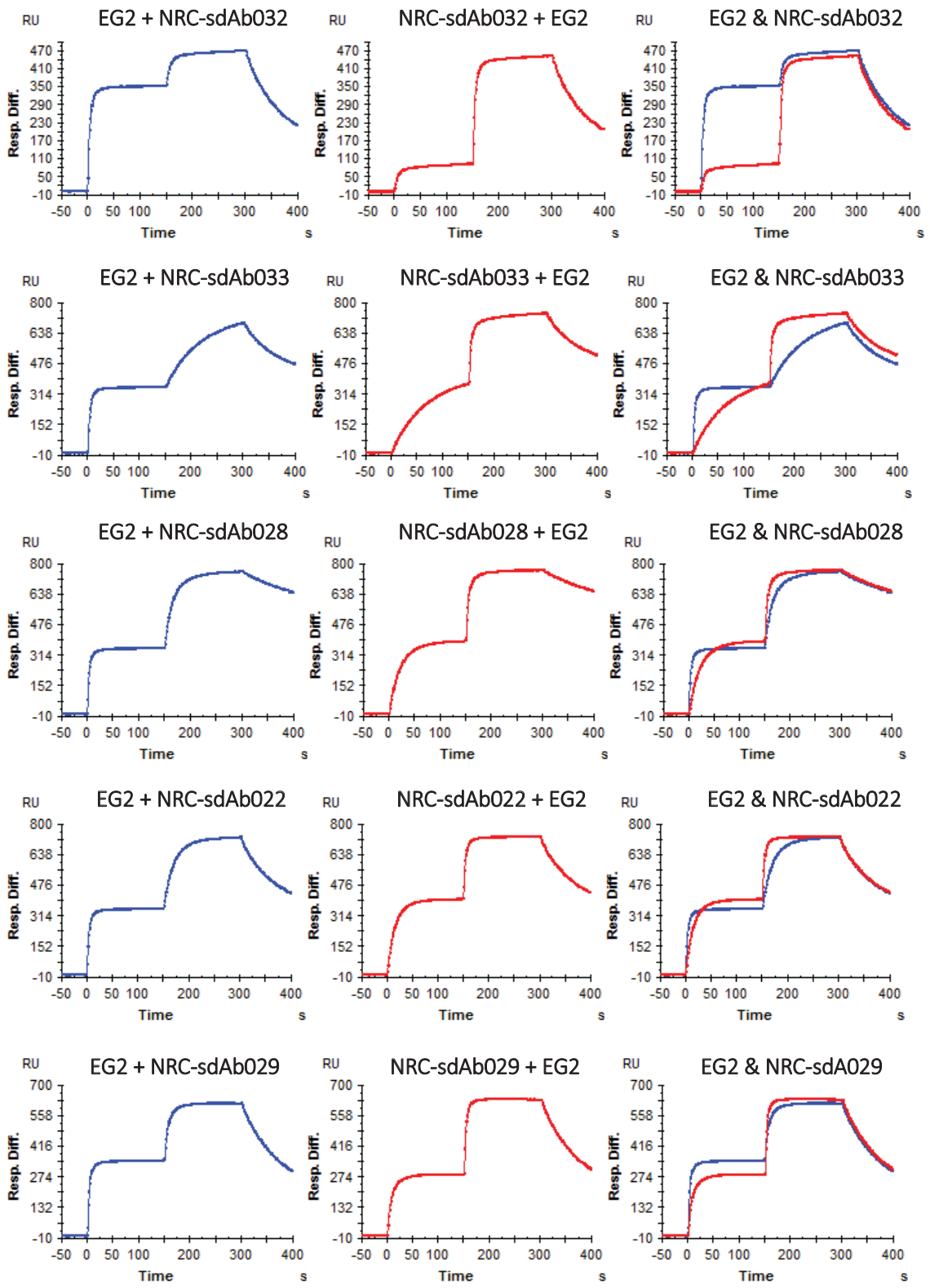
EG2 + NRC-sdAb032
NRC-sdAb032 + EG2
EG2 & NRC-sdAb032
EG2 + NRC-sdAb033
NRC-sdAb033 + EG2
EG2 & NRC-sdAb033
EG2 + NRC-sdAb028
NRC-sdAb028 + EG2
EG2 & NRC-sdAb028
EG2 + NRC-sdAb022
NRC-sdAb022 + EG2
EG2 & NRC-sdAb022
EG2 + NRC-sdAb029
NRC-sdAb029 + EG2
EG2 & NRC-sdA029
RU
Resp. Diff.
Time
s

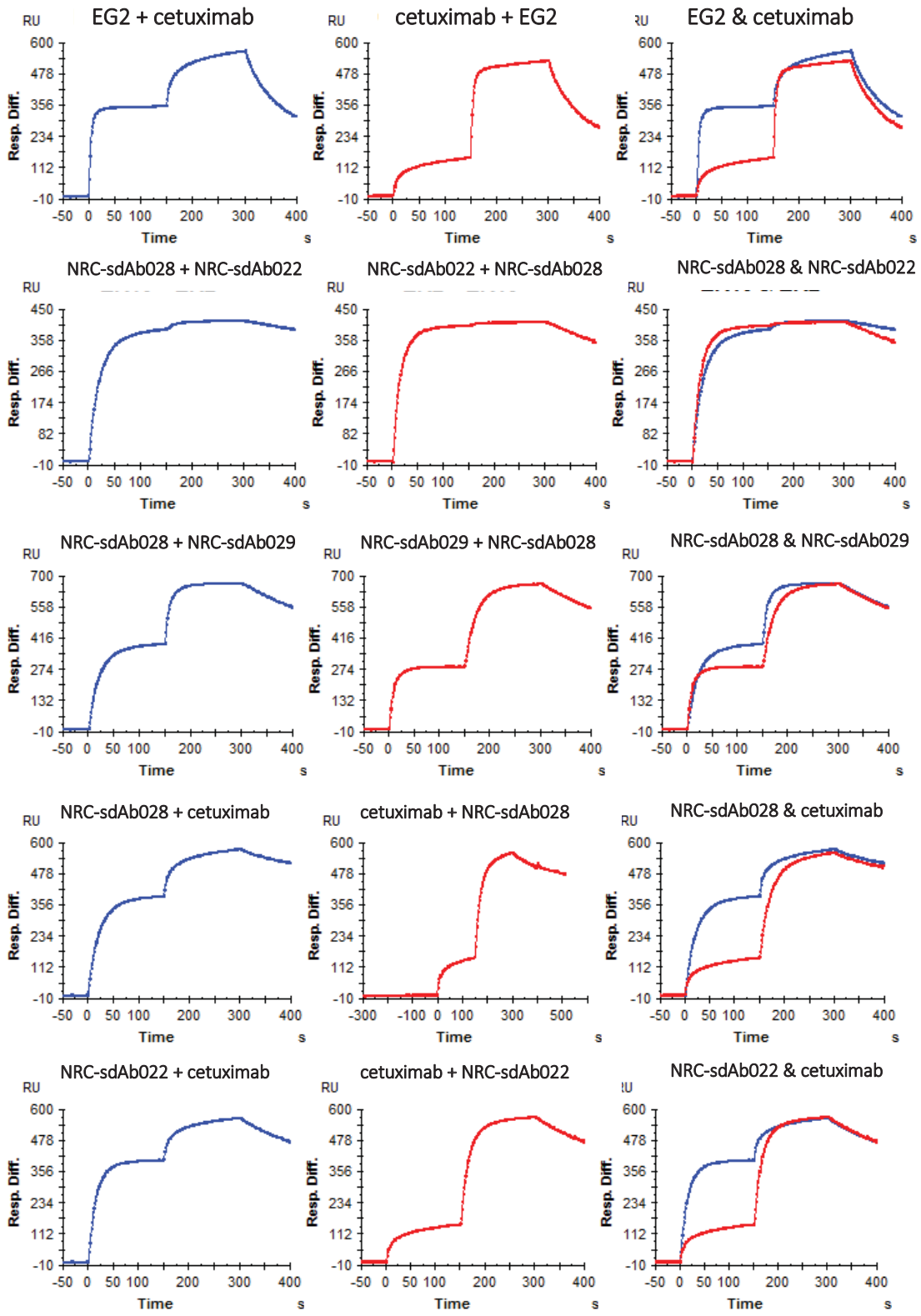
EG2 + cetuximab
cetuximab + EG2
EG2 & cetuximab
NRC-sdAb028 + NRC-sdAb022
NRC-sdAb022 + NRC-sdAb028
NRC-sdAb028 & NRC-sdAb022
NRC-sdAb028 + NRC-sdAb029
NRC-sdAb029 + NRC-sdAb028
NRC-sdAb028 & NRC-sdAb029
NRC-sdAb028 + cetuximab
cetuximab + NRC-sdAb028
NRC-sdAb028 & cetuximab
NRC-sdAb022 + cetuximab
cetuximab + NRC-sdAb022
NRC-sdAb022 & cetuximab
RU
Resp. Diff.
Time
s

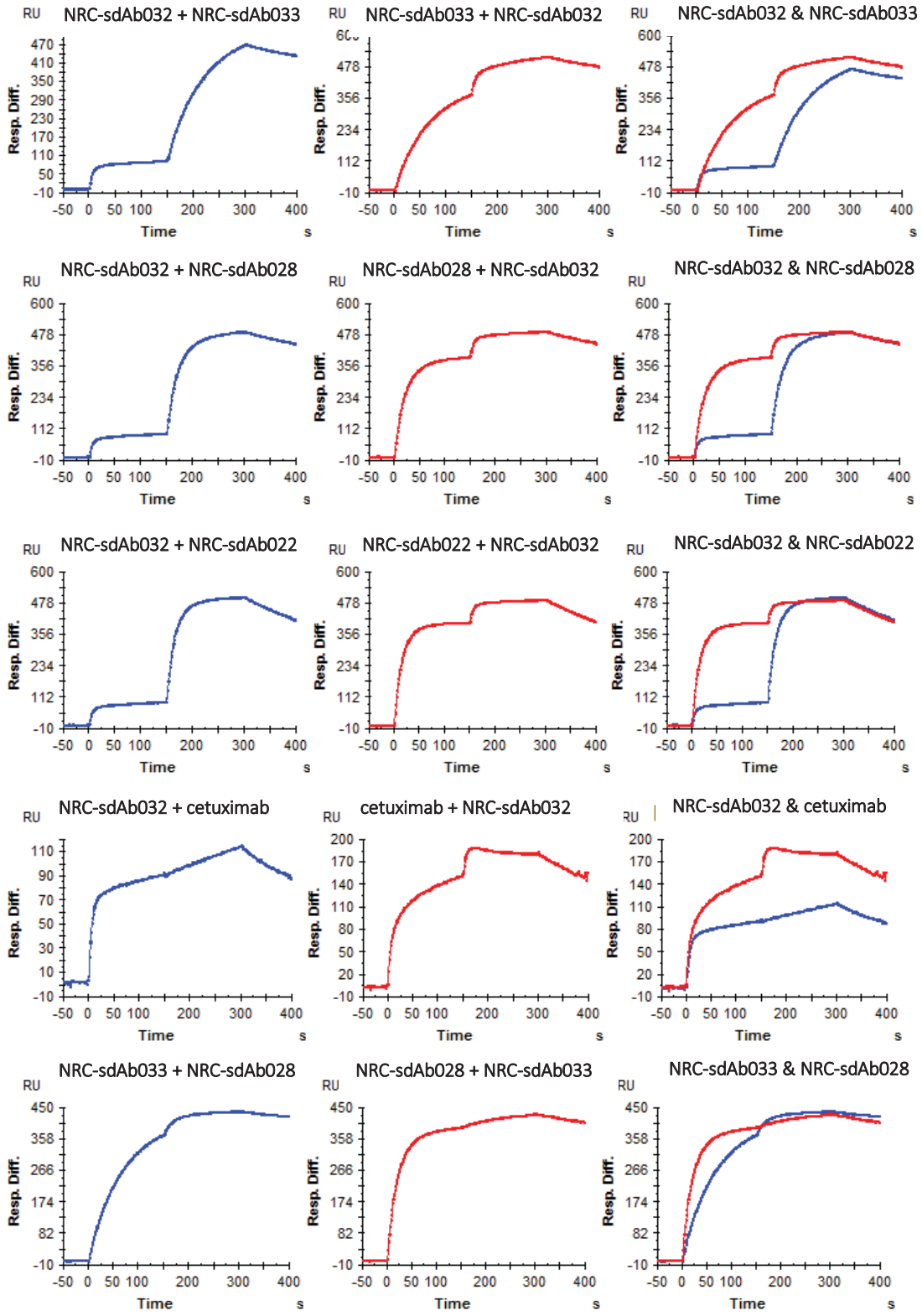
NRC-sdAb032 + NRC-sdAb033
NRC-sdAb033 + NRC-sdAb032
NRC-sdAb032 & NRC-sdAb033
NRC-sdAb032 + NRC-sdAb028
NRC-sdAb028 + NRC-sdAb032
NRC-sdAb032 & NRC-sdAb028
NRC-sdAb032 + NRC-sdAb022
NRC-sdAb022 + NRC-sdAb032
NRC-sdAb032 & NRC-sdAb022
NRC-sdAb032 + cetuximab
cetuximab + NRC-sdAb032
NRC-sdAb032 & cetuximab
NRC-sdAb033 + NRC-sdAb028
NRC-sdAb028 + NRC-sdAb033
NRC-sdAb033 & NRC-sdAb028
RU
Resp. Diff.
Time
s

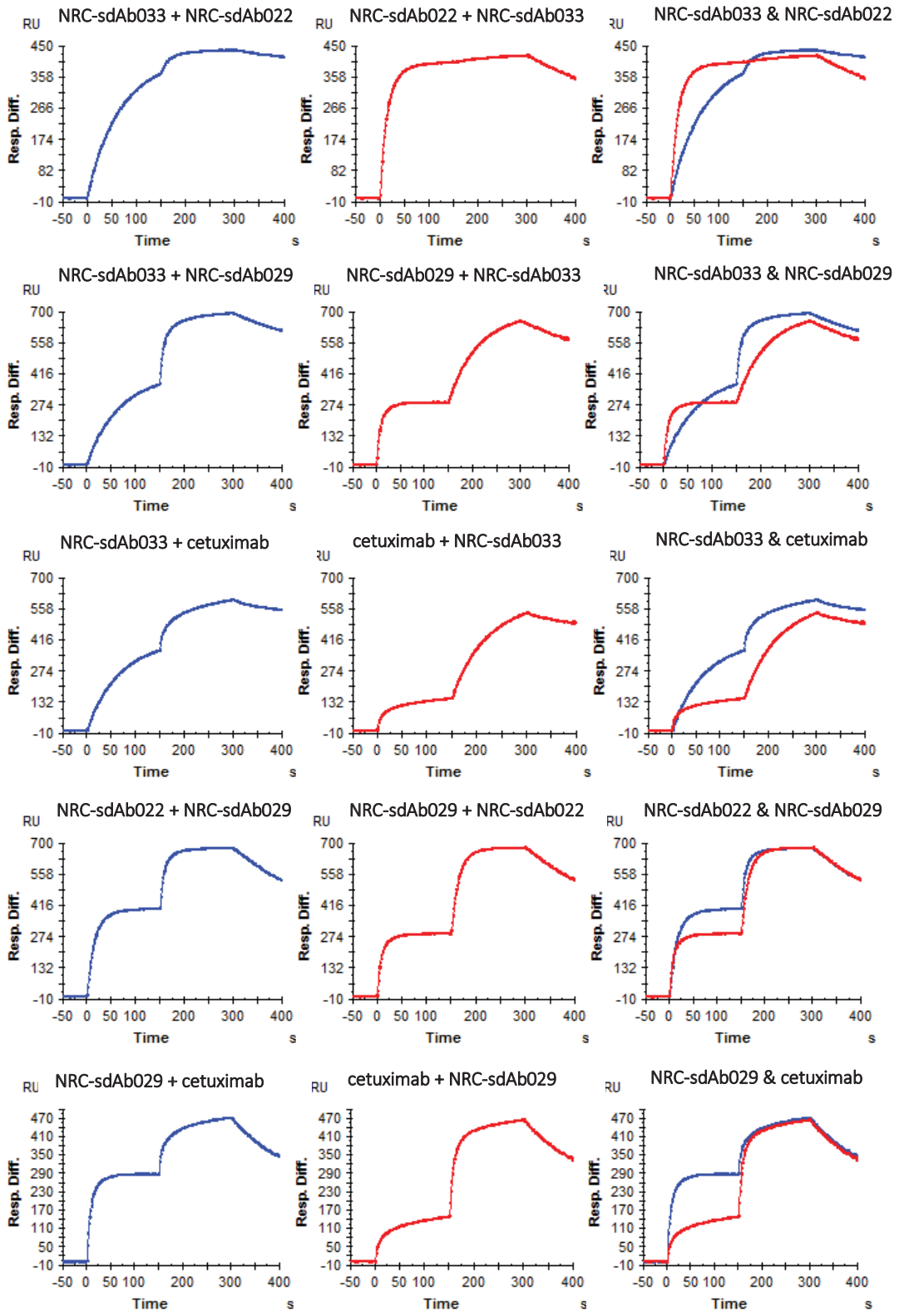
NRC-sdAb033 + NRC-sdAb022
NRC-sdAb022 + NRC-sdAb033
NRC-sdAb033 & NRC-sdAb022
NRC-sdAb033 + NRC-sdAb029
NRC-sdAb029 + NRC-sdAb033
NRC-sdAb033 & NRC-sdAb029
NRC-sdAb033 + cetuximab
cetuximab + NRC-sdAb033
NRC-sdAb033 & cetuximab
NRC-sdAb022 + NRC-sdAb029
NRC-sdAb029 + NRC-sdAb022
NRC-sdAb022 & NRC-sdAb029
NRC-sdAb029 + cetuximab
cetuximab + NRC-sdAb029
NRC-sdAb029 & cetuximab
RU
Resp. Diff.
Time
s

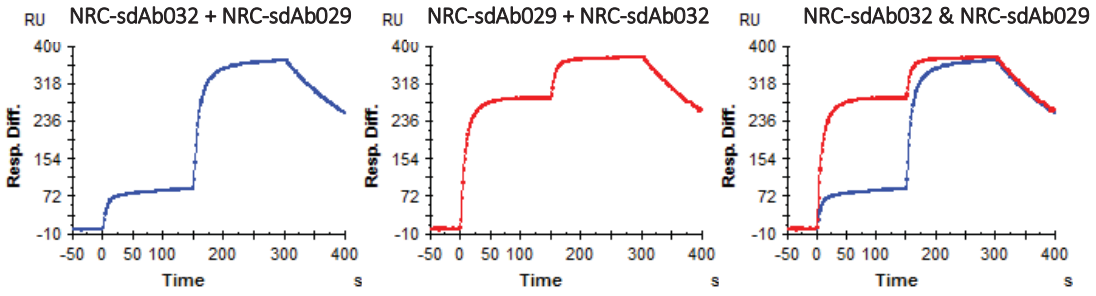

Supplementary Figure S2. Sensorgrams for all epitope binning SPR co-injection experiments. One representative of each V_HH family elicited by DNA immunization was selected (NRC-sdAb022, NRC-sdAb028, NRC-sdAb029, NRC-sdAb032, NRC-sdAb033) along with EG2 V_HH and cetuximab. In the first injection, the EGFR surface was saturated using a concentration equivalent to 25× K_D of the first antibody, then in the second injection, the first antibody was supplied in the presence of a second antibody (also 25× K_D) to determine whether additional binding occurred. All possible permutations of antibodies were tested as described in the main text.

Supplementary Table S1. Sequence characteristics of anti-EGFR V_HHs raised by llama DNA immunization.

Family	V_HH	CDR-H3 Length (aa)[a]
-	EG2	18
1	NRC-sdAb021	8
	NRC-sdAb022	8
	NRC-sdAb023	8
	NRC-sdAb024	8
	NRC-sdAb025	8
	NRC-sdAb026	8
	NRC-sdAb027	8
2	NRC-sdAb028	10
3	NRC-sdAb029	17
	NRC-sdAb030	17
4	NRC-sdAb032	12
5	NRC-sdAb033	11

[a]IMGT definition

Supplementary Table S2. Sequence characteristics of humanized anti-EGFR V_HHs.

V_HH	No. of amino acid changes with respect to parent	Overall amino acid identity with human IGHV3-30 (%)	Framework region amino acid identity with human IGHV3-30 (%)[a]
NRC-sdAb022	0	71.3	77.5
NRC-sdAb022-H1	12	83.0	91.3
NRC-sdAb022-H2	14	85.1	93.8
NRC-sdAb022-H3	17	88.3	97.5
NRC-sdAb028	0	72.6	76.3
NRC-sdAb028-H1	10	82.1	88.8
NRC-sdAb028-H2	13	85.3	92.5
NRC-sdAb028-H3	17	89.5	97.5
NRC-sdAb032	0	67.4	75.0
NRC-sdAb032-H1	13	80.0	91.3
NRC-sdAb032-H2	16	83.2	95.0
NRC-sdAb032-H3	18	85.3	97.5
NRC-sdAb033	0	67.4	75.0
NRC-sdAb033-H1	12	79.0	90.0
NRC-sdAb033-H2	15	82.1	93.8
NRC-sdAb033-H3	18	85.3	97.5

[a]IMGT framework definitions